

Trapping Induced N_{eff} and Electrical Field Transformation at Different Temperatures in Neutron Irradiated High Resistivity Silicon Detectors*

V. Eremin⁺, Z. Li, and I. Iljashenko⁺

Brookhaven National Laboratory, Upton, NY 11973-5000, USA

+ Permanent address: A. F. Ioffe Physico-Technical Institute of Academy of Sciences of Russia, St. Petersburg, Russia

Abstract

The trapping of both non-equilibrium electrons and holes by neutron induced deep levels in high resistivity silicon planar detectors have been observed. In the experiments Transient Current and Charge Techniques, with short laser light pulse excitation have been applied at temperature ranges of 77-300 K. Light pulse illumination of the front (p^+) and back (n^+) contacts of the detectors showed effective trapping and detrapping, especially for electrons. At temperatures lower than 150 K, the detrapping becomes non efficient, and the additional negative charge of trapped electrons in the space charge region (SCR) of the detectors leads to dramatic transformations of the electric field due to the distortion of the effective space charge concentration N_{eff} . The current and charge pulses transformation data can be explained in terms of extraction of electric field to the central part of the detector from the regions near both contacts. The initial field distribution may be recovered immediately by dropping reverse bias, which injects both electrons and holes into the space charge region. In the paper, the degree of the N_{eff} distortions among various detectors irradiated by different neutron fluences are compared.

I. Introduction

This work, carried out under a joint program of the collaboration between BNL and PTI, presents the novel results of recent investigations on radiation induced

MASTER

2

DISTRIBUTION OF THIS DOCUMENT IS UNLIMITED

degradation's of silicon planar detectors. In the field of neutron radiation problem of silicon detectors, majority of the efforts has been directed to such applied aspects as the transformation of current-voltage and capacitance-voltage characteristics and increase of detector full depletion voltage V_d and its annealing with neutron fluence at working temperatures $\sim 270-300$ K (0°C to room temperature (RT))[1-3], and charge collection efficiency at RT[4]. At the same time, phenomena such as trapping as well as detrapping of carriers from neutron induced deep levels at various temperatures have not been investigated so completely. For practical purposes, cooling has been applied to the detectors to low the leakage current and freeze the V_d reverse annealing[3]. At low temperature conditions, however, the trapping and detrapping of deep levels may cause unpredictable modifications of detector electrical properties such as the effective concentration of ionized charges in space charge region (N_{eff}), which would in turn modify the electrical field distribution and therefore affect the detector charge collection property.

In this work, the study of kinetics of non equilibrium carriers transport in neutron irradiated detectors is presented. The transport phenomena is investigated, using a laser transient current technique (TCT), in the temperature range of 110 to 310 K. The data allows one to propose a physical model which describes the observed transformation of electric field distribution with temperature inside the detector and some peculiarities in the kinetics of charge collection.

II. Samples and Experimental Technique

Planar p^+-n-n^+ detectors produced in BNL from $5\text{ k}\Omega\text{-cm}$ n-type silicon wafers (thickness $350\text{ }\mu\text{m}$, area $3\times 3\text{ mm}^2$) have been irradiated by 1 MeV neutrons to fluences in the range of 10^{13} to 10^{14} n/cm^2 . The block diagram of the TCT set up and the cryostat is shown in Fig. 1. The sample was assembled on the cooper table with heater and

temperature control thermocouple, and the whole assembly was put inside a metal chamber. The chamber was covered by the glass bell protecting the chamber from a direct contact with liquid nitrogen surrounding it. The sample was AC coupled with high frequency oscilloscope TDS-445 (Textronix) by thin coaxial cable. Non equilibrium carriers were generated by a GaAs laser with wave length of $\sim 0.8\mu\text{m}$ and light pulse duration of ~ 1 ns. The diameter of laser illumination spot on the detector is ~ 2 mm. The laser was pumped by nanoseconds current pulses from a pulse generator through a current amplifier. To shift response pulse in time with respect to the triggering of the oscilloscope and to decrease the ripples induced by current pulse pampering, an optic delay line has been used. As the optic fiber used in the existing set-up showed a strong dependence of transmission efficiency on temperature in region below 230 K, the part of optic fiber which might be cooled inside cryostat was surrounded by a temperature controlled heater. This allows the maintenance of the energy of laser pulse deposit on the sample to an accuracy better than 1% at temperatures ranging from RT to 100 K. This set-up allows one to analyze detector waveforms of current pulses with amplitude as small as ~ 1 mV, that corresponds to the generation of about 2×10^6 electron-hole pairs.

TCT measurements of current pulses have been made at different temperatures starting from 320 K down to 100 K, with equal time interval between each measurement to ensure the same quasi-steady state condition. The current shapes were stored in the floppy diskettes and later treated by special software.

III. Experimental Results

In this section we present and analyze the temperature dependence of current shapes for two detectors irradiated by two different fluences near and after the SCR inversion. For the sample irradiated to lower fluence (2.3×10^{12} n/cm², 15 months after radiation), the electron current shapes (laser illumination on the front side or p⁺ contact) at a bias of 50 volts and at temperatures from RT to 170 K are shown in Fig. 2. This

detector has been found to fully deplete at a voltage of less than 15 volts, corresponding to a N_{eff} of less than $4.65 \times 10^{10} / \text{cm}^3$.

Let us consider transformation of current shapes with temperature. As it is known, the current pulse form is determined by two main factors:

- the value of carrier mobility
- electric field distribution related with the value and profile of N_{eff} .

At temperatures below 300 K but above 220 K (see Fig. 2a), the pulses conserve their forms in general. The main changes were related to mobility increasing with the cooling of the detectors. Dramatic transformations of current shapes start to take place at $T \cong 200$ K, as shown in Fig. 2b. As we follow the sequences of current shapes in Fig. 2b, the slope of current shape is practically flat at $T=200$ K and starts to increase at lower temperatures, indicating that the maximum of electrical field is now shifting from the p^+ contact before transformation to the n^+ contact. This electrical field transformation is a result of the change of the sign of N_{eff} in the SCR from positive to negative. Fig. 3 shows the detector hole current shapes (laser illumination on the back side or n^+ contact) at same bias and temperature conditions as shown in Fig. 2. Again the trend of carrier mobility increase with temperature is the same as in the electron current case. Same transformation trend of current shape top has been observed. However, since holes drift from the back contact towards the front contact, the maximum field stays at the front contact, as compared to shifting from front contact to back contact in the case of electron current shape. In the hole current case, the N_{eff} is positive and increases with decreasing temperature. Note here that in both cases, the sign of the N_{eff} after the transformation is the same as that of the moving free carriers.

Another important effect associated with current shape transformation is that the degradation of the area of current pulse at lower temperatures than 180 K. This degradation of area correlates with appearance of a long tail on the current pulses (Fig. 2b and Fig. 3b) It needs to point out, that a slow component of current pulse is often

observed in the current and charge responses of partially depleted p^+-n-n^+ -detectors in cases when the conductivity of neutral base is low enough to contribute appreciable ohmic current[5-7]. The time constant, however, of this ohmic current is in the order of μs for temperatures higher than 260 K, and it increases with the reciprocal of temperature . So, at $T \sim 200$ K, its value must be much larger than the duration of observed slow component (in the order of tens of ns).

It is clear that the above presented current shape transformations, including the change of electrical field profile and the degradation of amplitude, are very complicated and are specific peculiarities for irradiated detectors working at low temperatures. In the next section, we will propose a model that will describe the observed effects in terms of free carrier-deep level interaction.

IV. Model

The diagrams of N_{eff} and field distributions, for an irradiated but not inverted silicon detector, illustrating the proposed model are shown in Fig. 4. The distributions at room temperature are standard and are shown in Fig. 4a corresponding with the current pulse in Fig. 2a and 3a. Let us consider the case of laser illumination on the p^+ -contact. Decreasing of temperature leads to changing of balance between rates of trapping and detrapping of drifting electrons. As trapping time constant τ_t decreases with decreasing temperature in the form:

$$\tau_t = \frac{1}{\sigma v_t(T) N_t} \quad (1)$$

where σ is the trapping cross section of the deep level, $v_f(T)$ is the thermal velocity and N_f is the concentration of the deep level. The detrapping time constant τ_d is more strongly dependent on the temperature:

$$\tau_d = \frac{1}{\sigma v_f N_C(\text{or } N_V) \cdot e^{-\frac{E_f}{kT}}} \quad (2)$$

and it decreases exponentially with cooling. In the equation, N_C is the density of states in conduction (N_V for valence) band, E_f is the activation energy for detrapping, and k is the Boltzmann constant.

Therefore the steady-state balance of trapped and detrained charges is shifting more and more towards the trapping with decreasing temperature. In other words, the trapped charges are frozen in deep levels at low temperatures. In the case of electron drifting in the SCR, electron trapping progress may lead to conversion from the initial positive space charge into negative, as illustrated in Fig. 4b-4d. Accordingly, the maximum of the electrical field shifts from the p^+ contact to n^+ contact, in agreement with the observed current shape shown in Fig. 2.

Similarly, in the case of hole drifting in the SCR, trapped holes would increase the initial positive space charge concentration, which leads to even higher electrical field maximum at the n^+ contact in agreement with data shown in Fig. 3. Note in both cases, the electrical field minimums are on the side of the illuminated contacts after the transformation.

Obviously in both cases after the transformation, the absolute values of the space charge concentration N_{eff} may be larger than the initial one and the junction is on the side opposite of the laser generated free carries. For a given bias enough to deplete the detector before the transformation, the detector may become partially depleted due to the N_{eff} increase. This would leave, as shown in Fig. 4e and 4h, only part of the distribution of

generated free carriers (or namely, the tail) in the drifting electrical field, leading to the decrease of the current pulse amplitude and the area of the current pulse fast component. The generated free carriers in the neutral region (no field region) may still contribute to the current pulse by means of diffusion to the border of the SCR leading to the appearance of current pulse tail.

The average duration of this diffusion process can be estimated as

$$\tau_{diff} = \frac{\Delta^2}{D} \quad (3)$$

where D is the diffusion coefficient of free carriers and Δ is the thickness of the neutral region.

Let us estimate the values of t_{diff} for both electrons and holes. At $T \sim 200$ K and $\Delta \sim 10 \mu\text{m}$, the diffusion time is about 15 ns for electrons and 40 ns for holes, in agreement with the observed tails shown in Fig. 2b and Fig. 3b.

As for the decrease of the area of the fast component of the current pulse (or the drifting current), it can be estimated as the following:

$$Q_f = q_0 - \int_0^{\Delta} \frac{q_0}{\lambda} \cdot e^{-\frac{x}{\lambda}} dx \quad (4)$$

where Q_f is the charge collected in the fast component, q_0 is the total generated charge, and λ is the absorption length of the laser light in the detector.

The qualitative considerations described above allow us to construct the mathematical model of the transformation of electrical field in the SCR determine the time when the area degradation start to take place. The Poisson and continuity equation describing the carrier transport in the bulk of the detector are non linear differential

equations which can not be solved analytically. However, analytical solutions can be obtained with the following simplifications:

- the distribution of N_{eff} in the SCR stays uniform at all times.
- the concentration of the moving carriers is a constant over the SCR.

With the conditions listed above, the changes of the space charge density N_{eff} due to the trapping and detrapping of moving free electrons (p^+ illumination) can be described as:

$$\frac{dN_{eff}}{dt} = \frac{dn_t}{dt} = \frac{n}{\tau_t^e} - \frac{n_t}{\tau_d^e} \quad (5)$$

where n_t and n are density of trapped carriers and free carriers in the bulk of SCR, respectively, and τ_t^e and τ_d^e are trapping and detrapping time constants for electrons defined previously in eq. (1) and (2), respectively.

Combining eq. (1), (2), and (5), we get:

$$\begin{cases} \frac{dn_t}{dt} = -\left(n\sigma v_t + \frac{1}{\tau_d^e}\right)n_t + n\sigma v_t N_t \\ n_t(t=0) = 0 \end{cases} \quad (6)$$

The analytical solutions of eq. (6) can be written as:

$$\begin{cases} n_t(t) = \frac{n\sigma v_t N_t}{n\sigma v_t + 1/\tau_d^e} \cdot \left[1 - e^{-\frac{t}{\tau_{trans}}}\right] \\ \tau_{trans} = \frac{1}{n\sigma v_t + 1/\tau_d^e} \end{cases} \quad (7)$$

where τ_{trans} is defined as the transformation time constant.

Similarly, in the case of hole drifting in the SCR (n^+ contact illumination), the concentration of trapped holes is:

$$\begin{cases} p_t(t) = \frac{p\sigma v_t N_t}{p\sigma v_t + 1/\tau_d^h} \cdot \left\{ 1 - e^{-\frac{t}{\tau_{trans}}} \right\} \\ \tau_{trans} = \frac{1}{p\sigma v_t + 1/\tau_d^h} \end{cases} \quad (8)$$

where p is the concentration of generated free holes in the SCR and τ_d^h is the detrapping time constant for holes.

The total concentration of the space charge N_{eff} is now changed to :

$$\begin{cases} N_{eff}(t) = N_{eff}^0 - n_t(t) & (p^+ \text{ illumination}) \\ N_{eff}(t) = N_{eff}^0 + p_t(t) & (n^+ \text{ illumination}) \end{cases} \quad (9)$$

where N_{eff}^0 is the initial concentration of space charge before the transformation. It is clear that, if the concentrations of trapped carriers are higher than the initial concentration of space charge which is assumed positive here, N_{eff} would transform from positive to negative (or "n" to "p" inversion in the SCR) in the case of p^+ illumination, and it would become more positive in the case of n^+ illumination, in exact agreement with the data shown before.

Further examination of eq. (7) and (8) shows that (for simplicity, we use n_0 as the symbol for n and p , i.e. $n_0 = n$ or p accordingly):

a) at longer time ($t \gg \tau_d$ and τ_{trans}), the steady state concentration of trapped carriers is:

$$n_t^{\max}, p_t^{\max} = \frac{n_0 \sigma v_t N_t}{n_0 \sigma v_t + 1/\tau_d^{e,h}} \quad (10)$$

According to eq. (9), n_t^{\max} and p_t^{\max} are the upper limits of the net change of the N_{eff} .

$$|\Delta N_{eff}^{\max}| = n_t^{\max} \text{ or } p_t^{\max} \quad (11)$$

and $|\Delta N_{eff}^{\max}|$ is therefore affected by the generated free carrier concentration n_0 , the total deep level concentration N_t which is proportional to the neutron fluence Φ_n , and the temperature via the dependence of $\tau_d(T)$ expressed in eq. (2). At low temperatures ($\tau_d(T) \gg 1/(n_0 \sigma v_t)$):

$$n_t^{\max}, p_t^{\max} \cong N_t \quad (12)$$

N_{eff} transformation is at its maximum.

At high temperatures ($\tau_d(T) \ll 1/(n_0 \sigma v_t)$):

$$n_t^{\max}, p_t^{\max} \cong \tau_d \cdot (n_0 \sigma v_t) \cdot N_t \ll N_t \quad (13)$$

there is no or little N_{eff} transformation.

This point is clearly shown in Fig. 5, where the concentrations of trapped carriers at various temperatures are plotted against the time using eq. (7) or (8).

b) The transformation time constant τ_{trans} is dependent on the generated free carrier concentration n_0 and the temperature (through $\tau_d(T)$). At high temperatures, τ_{trans} depends strongly on the generated free carrier concentration:

$$\tau_{trans} \cong \frac{1}{n_0 \sigma v_t} \quad (14)$$

We note here that n_0 is a general term of generated free carriers which includes laser (or other sources) generated carriers as well as thermally generated carriers in leakage current.

Let us now consider the timing of the current pulse amplitude and area degradations. According to the model described previously, the electric field near the contact of laser illumination approaches zero at the start of the amplitude and area degradations. In other words, the degradations start at the time when a full depletion is reached:

$$|N_{eff}(t)| = \frac{2\epsilon\epsilon_0 V}{ed^2} \quad (15)$$

where d is the detector thickness.

Combining eq.(7), (8) and (15), we get the equation which describes the relation between properties of material in SCR and the timing for detector current amplitude and area degradations τ_{deg} :

$$\frac{2\epsilon\epsilon_0 V}{ed^2} = \left| N_{eff}^0 \pm N_t \frac{1}{1 + \frac{1}{n_0 \sigma v \tau_d^{e,h}}} \left\{ 1 - e^{-\frac{\tau_{deg}}{\tau_{trans}}} \right\} \right| \quad (16)$$

where - sign is for electron drifting (p^+ contact illumination, τ_d^e), and + sign is for hole drifting (n^+ contact illumination, τ_d^h). The temperature dependence of the detrapping time constants has been expressed previously in eq.(2).

From eq. (16), we can solve the degradation time constant τ_{deg} in terms of τ_{trans} , n_t^{\max} or p_t^{\max} , and V and d as the following:

$$\tau_{deg} = -\tau_{trans} \cdot \begin{cases} \ln \left[1 - \left(\frac{2\epsilon\epsilon_0 V}{ed^2} + N_{eff}^0 \right) / n_t^{\max} \right] & \text{(Electron current)} \\ \ln \left[1 - \left(\frac{2\epsilon\epsilon_0 V}{ed^2} - N_{eff}^0 \right) / p_t^{\max} \right] & \text{(Hole current)} \end{cases}$$

$$n_t^{\max} > \frac{2\epsilon\epsilon_0 V}{ed^2} + N_{eff}^0, p_t^{\max} > \frac{2\epsilon\epsilon_0 V}{ed^2} - N_{eff}^0 \quad (17)$$

where the sign of N_{eff}^0 can be positive ("n" SCR) and negative ("p" SCR) and the voltage was chosen such that $|N_{eff}^0| < 2\epsilon\epsilon_0 V / ed^2$.

Fig. 6 illustrates the transformation of current pulses as a function of time or the non-steady state transformations. The current pulses in Fig. 6a were recorded in every 10 seconds and those in Fig. 6b were recorded in every 20 seconds. In both cases the processes of field transformations are analogous in general, but have a difference in transformation timing. The current response shows the transition period with non regular field distribution which correspond accumulation of opposite charges near the detector contacts separated by intrinsic region.

As it can be seen, the rate of the degradations of the current pulse amplitude and area is determined not only by the properties of deep levels (N_t, σ, E_t), but also the free carrier concentration in the SCR. The free carriers can be supplied by the bulk leakage current (thermally generated carriers) and current of laser generated carriers (externally generated carriers). At low temperatures ($T \sim 200$ K), the leakage current for detectors irradiated to a few times of 10^{12} n/cm² does not exceed the value $\sim 10^{-11}$ A[5] and free carriers concentration is:

$$n_{0,L} \cong \frac{I_L}{e\mu E \cdot A} \cong \frac{10^{-11}}{1.6 \cdot 10^{-19} \cdot 1.5 \times 10^6 \cdot 0.25} \cong 166 \text{ cm}^{-3} \quad (18)$$

where A is the detector area.

At the same time, the concentration of laser generated carriers at our experimental conditions (the frequency of light pulses $f=100$ Hz; each pulse generates $\sim n^0=10^7$ pairs, light spot on the sample has area $\sim 1 \text{ mm}^2$, and the absorption length is about $20 \text{ }\mu\text{m}$) can be estimated:

$$n_{0,gen} \cong n^0 \cdot t_{dr} \cdot f \cdot \frac{1}{A \cdot \lambda} = 10^7 \cdot 10^{-8} \cdot 100 \cdot \frac{1}{10^{-2} \cdot 2 \times 10^{-3}} = 10^6 \text{ cm}^{-3} \quad (19)$$

The main factor of N_{eff} transformation at low temperatures is therefore laser (or externally) generated carriers.

Conclusion

We have designed a model to describe the degradations of neutron irradiated detectors at low temperatures. The model is in very good agreement with the observed irregularities such as the field (or N_{eff}) transformations and the current pulse amplitude and area degradation at low temperatures. These irregularities have been attributed to the steady state balance of trapping and detrapping of deep levels. At low temperatures, the dominant process is the trapping, which not only causes the well known effect of charge collection loss, but also affects the net concentration of the space charge N_{eff} .

The main effects of detectors irradiated to intermediate fluences (\sim a few times of 10^{13} n/cm^2) are thought to be caused by the trapping of externally generated free carriers and they occur at low temperatures. However, at high fluences ($>10^{14} \text{ n/cm}^2$), the detector leakage current may be high enough at RT to be a dominant part of the total generated carrier concentration n_0 . As we have discussed in the previous section, n_0 plays an important role in the field transformation and one may expect some near RT field irregularities for detectors irradiated to high neutron fluences. Fig. 7 shows the electron

current shapes (p^+ side illumination) of a detector irradiated to $7 \times 10^{14} \text{ n/cm}^2$. Two current peaks with about equal sizes appear in the RT current shape, a clear indication of high electrical fields on both sides of the detector, or junctions on both sides similar with the early observations of Li et al.[8] The leakage current of the detector is very high at 305 K, about 875 μA , and goes down quickly with decreasing temperature. As temperature going down, the high field on the n^+ side is also going down and disappears at $T=260 \text{ K}$ ($I_L=5.3 \mu\text{A}$). It seems that the trapping of thermally generated carriers in the leakage is the main cause of this field irregularity. The preliminary model is that a) the detector leakage current supplies more carriers than externally generated carries at temperatures near RT; and b) since all electrons have to go through the n^+ contact and all holes have to go through the p^+ contact and not vice versa, more electrons would be trapped near the n^+ contact and therefore make the region more negative in space charge (or more "p" type in SCR near n^+ contact) and more holes would be trapped near the p^+ contact and make it more positive in space charge (or more "n" type near p^+ contact). We will make more detail study of this effect and the results will be published elsewhere.

We shall point out here the applied aspect of the findings reported and described above. Although the operation of detectors at temperatures less than 200 K is out of the current interest for high energy physics, the same field transformations observed at low temperature for fluences $\sim 10^{13} \text{ n/cm}^2$ also appear near the room temperature for fluences $> 10^{14} \text{ n/cm}^2$. These field transformations may affect the real, near RT (0 °C to RT) applications of the silicon detectors in the future large Collider.

Acknowledgment

The authors are grateful to N. Stokan of PTI for his interest and support to this work. The authors would also like to thank E. Verbitskaya and A. Ivanov of PTI, H.W. Kraner of BNL, and G. Lindstroem and E. Fretwurst of the University of Hamburg for helpful discussions.

References

1. R. Wunstorf, M. Benkert, N. Claussen, N. Croitoru, E. Fretwurst, G. Lindstrom, and T. Schulz, "Results on Radiation Hardness of Silicon Detectors up to Neutron Fluence of 10^{15}n/cm^2 ," *Nucl. Instr. Meths.*, A315, 149 (1992)
2. K. Gill, G. Hall, s. Roe, S. Sotthibandhu, R. Wheadon, P. Giubellino, and L. Ramello, "Radiation Damage by Neutrons and Photons to Silicon Detectors, *Nucl. Instr. Meths.*, A322, 177 (1992)
3. H. J. Ziock, J. G. Boissevain, K. Holzscheiter, J. S. Kapustinsky, A. P. T. Palounek, W. E. Sondheim, E. Barberis, N. Cartiglia, J. Leslie, D. Pitzl, W. A. Rowe, M. F. W. Sadrozinski, A. Seiden, E. Spencer, J. a. Ellison, J. K. Fleming, S. Jerger, D. Joyce, C. Lietzke, E. Reed, S. J. Wimpenny, P. Ferguson, M. A. Frantschi, J. A. J. Matthews, and D. Skinner, "Temperature Dependence of Radiation Damage and Its Annealing in Silicon Detectors," *IEEE Trans. Nucl. Sci.*, Vol.40, No. 4, 344(1993).
4. H.W. Kraner, Z. Li, and E. Fretwurst, The use of the Signal Current Pulse Shape to Study the Internal Electrical Field Profile and Trapping effects in Neutron Damaged Silicon Detectors, Presented at the Sixth European Symposium on Semiconductor Detectors, Milan, Italy, Feb. 24-26, 1992, *Nucl. Instr. and Meth.*, A326 (1993) 350-356.
5. Z. Li, V. Eremin, N. Strokan, and E. Verbitskaya, Investigation of the Type Inversion Phenomena: Resistivity and Carrier Mobility in the Space Charge Region and Electrical Neutral Bulk in Neutron Irradiated Silicon p^+-n Junction Detectors, Presented at the IEEE Nucl. Sci. Symp, Orlando, FL, Oct. 25-31, 1992, *Trans. Nucl. Sci.* Vol. 40, No.4, 367(1993)
6. V. Eremin and Z. Li, "Determination of the Fermi Level Position for Neutron Irradiated High Resistivity Silicon Detectors and Materials Using the Transient Charge Technique(TChT)", BNL-60072, to be presented at the IEEE Nuclear and Space Radiation Effects Conference, Tucson, Arizona, July 18-22, 1994, to be published in the IEEE Transaction on Nuclear Science.
7. V. Eremin, N. Strokan, and E. Verbitskaya, and Z. Li, "The Development of Transient Current and Charge Techniques for Measurement of Effective Concentration of Ionized Space Charges (N_{eff}) of p-n Junction Detectors, BNL-60156, to be submitted to the *Nucl. Intrs. & Meth.*
8. Z. Li and H. W. Kraner, "Fast Neutron Damage Effects on High Resistivity Silicon Junction Detectors," BNL-46198, Proc. of the third Workshop on Radiation-induced and/or Process-related Electrically Active Defects in Semiconductor-

insulator Systems, Research Triangle Park, NC, Sept. 10-13, 59 (1991), J.
electronic Materials, Vol. 21, No. 7, 701(1992).

Figure Captions

- Fig. 1** Block diagram of the TCT set up and the cryostat.
- Fig. 2** The transformation of current pulses with temperatures for a detector (#296-A3) irradiated to $2.3 \times 10^{12} \text{ n/cm}^2$. The laser light was on the p^+ side (electron current).
- Fig. 3** The transformation of current pulses with temperatures for a detector (#296-A3) irradiated to $2.3 \times 10^{12} \text{ n/cm}^2$. The laser light was on the n^+ side (hole current).
- Fig. 4** The schematics of the proposed model of carrier trapping induced field and space charge density (eN_{eff}) transformations with temperature. a) the initial eN_{eff} is positive (before inversion in the SCR); b)-e) laser light on the p^+ side, and T going down; f)-h) laser on the n^+ side, and T going down.
- Fig. 5** Simulated dependence of the concentration of trapped charges on time at various temperatures.
- Fig. 6** The transformation of current pulses at a given temperature ($T=100 \text{ K}$) with time for a detector (A-3) irradiated to $5.5 \times 10^{12} \text{ n/cm}^2$. The laser light was on the n^+ side (hole current). The time interval between adjacent curves is a) 10 seconds; and b) 20 seconds.
- Fig. 7** The transformation of current pulses with temperatures for a detector (#436-85) irradiated to $3.1 \times 10^{14} \text{ n/cm}^2$. The laser light was on the p^+ side (electron current).

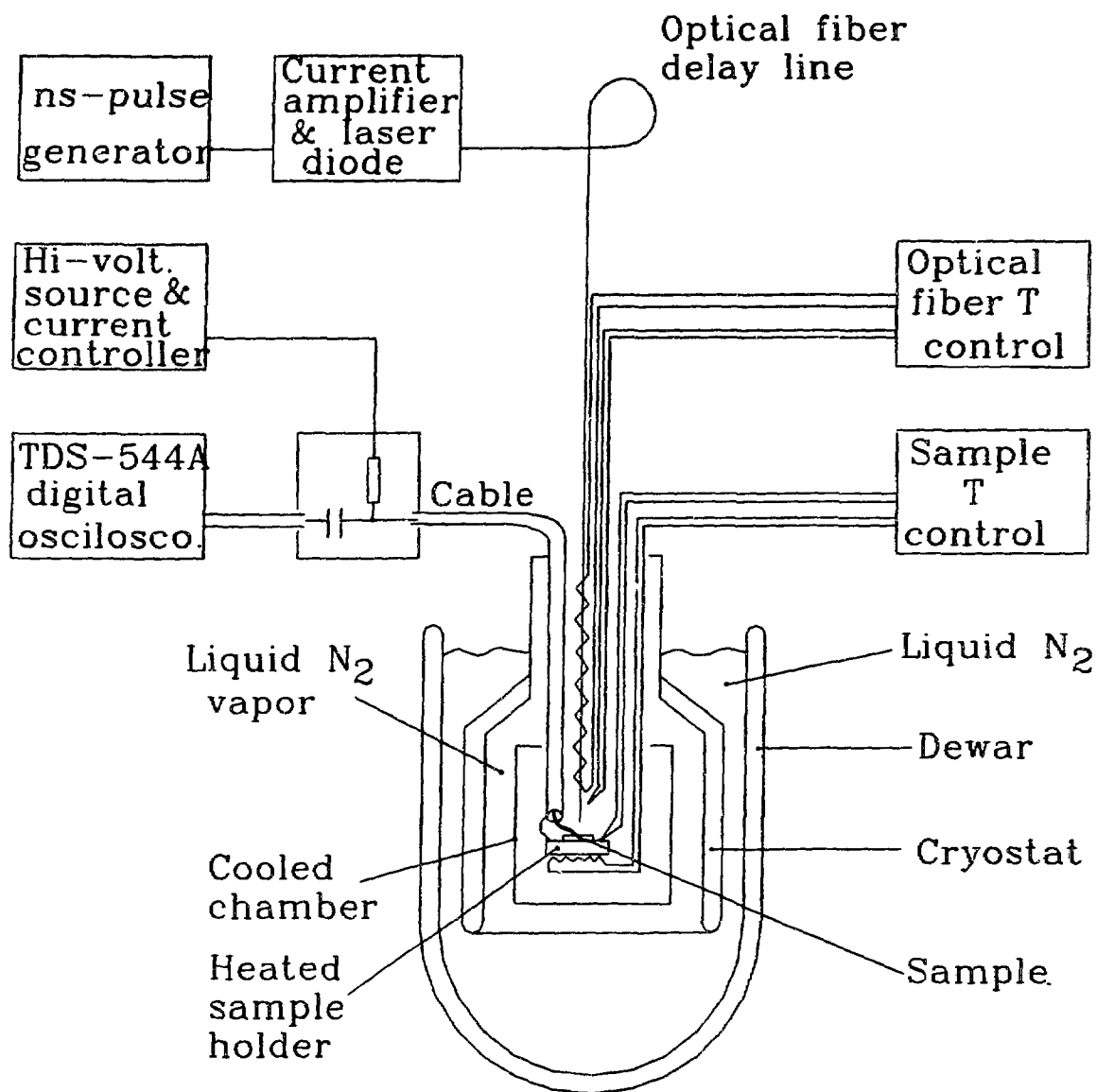
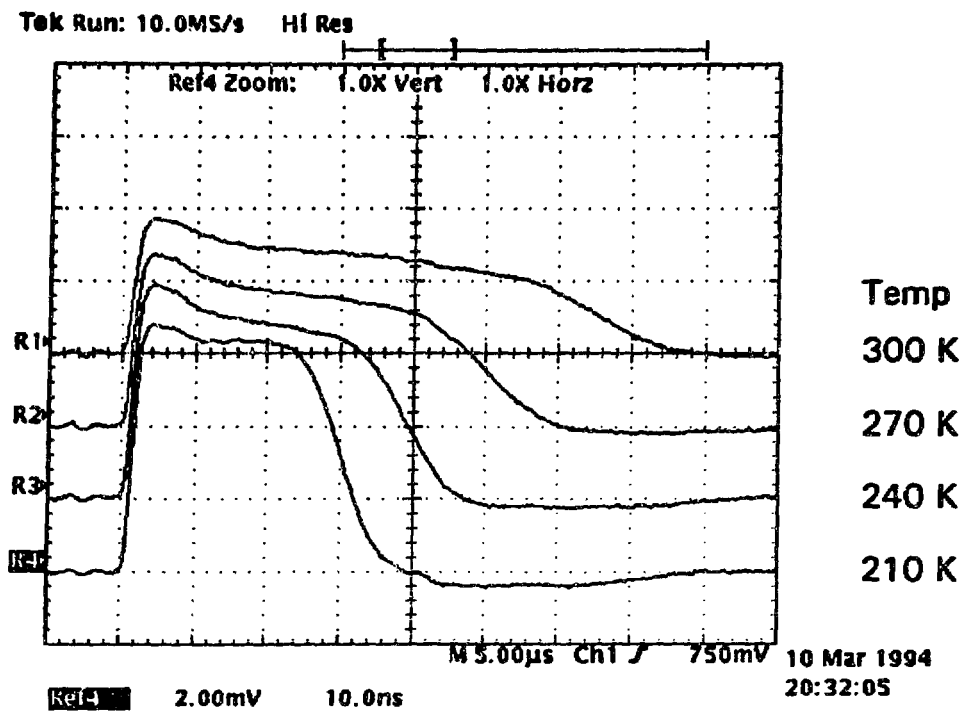
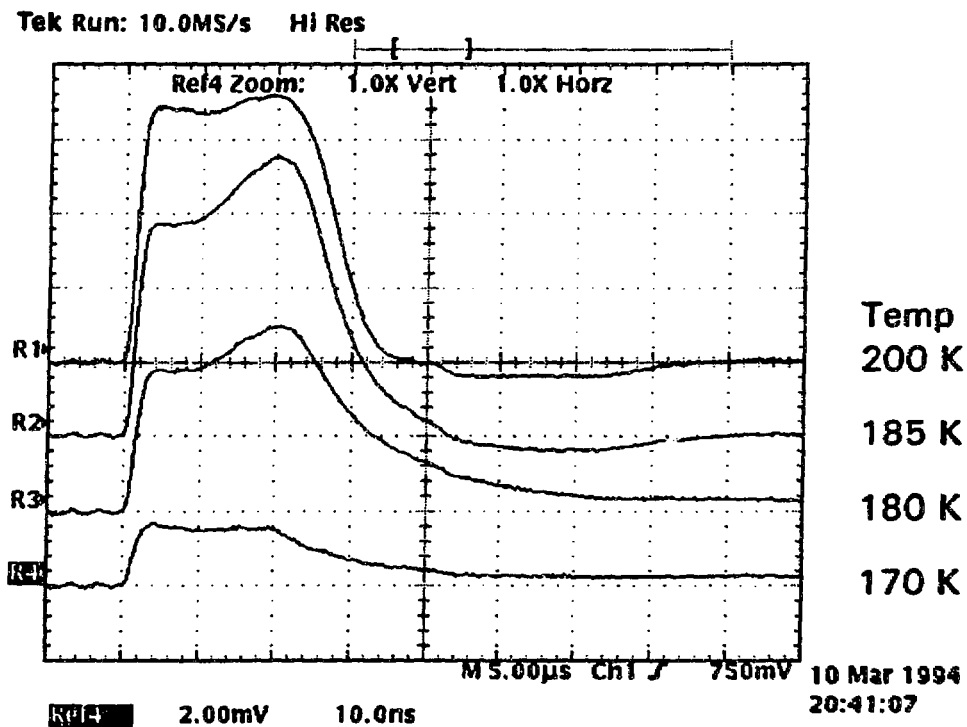


Figure 1



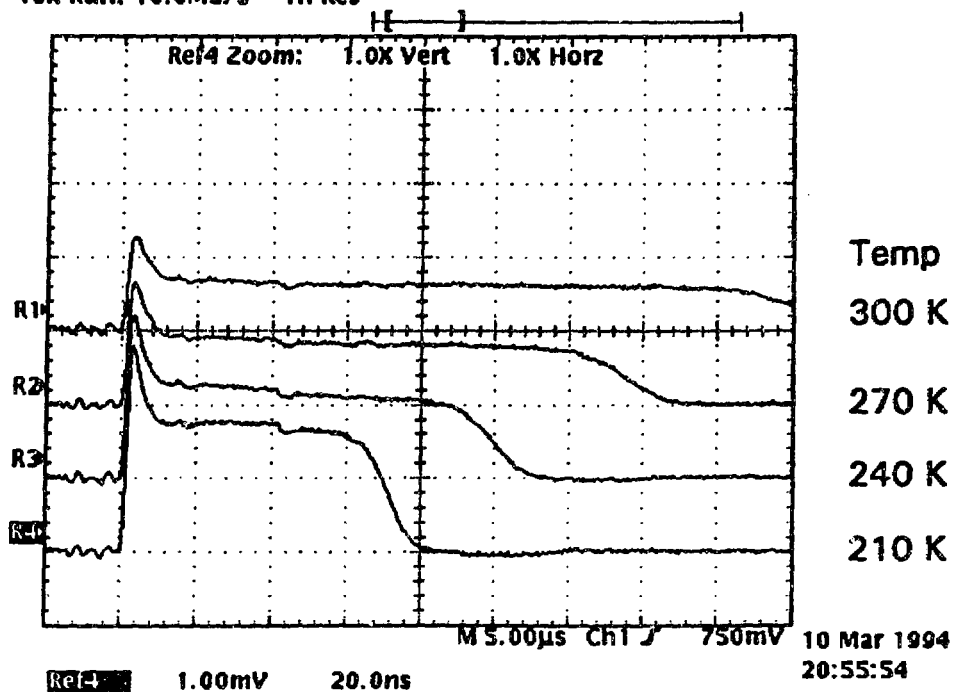
a)



b

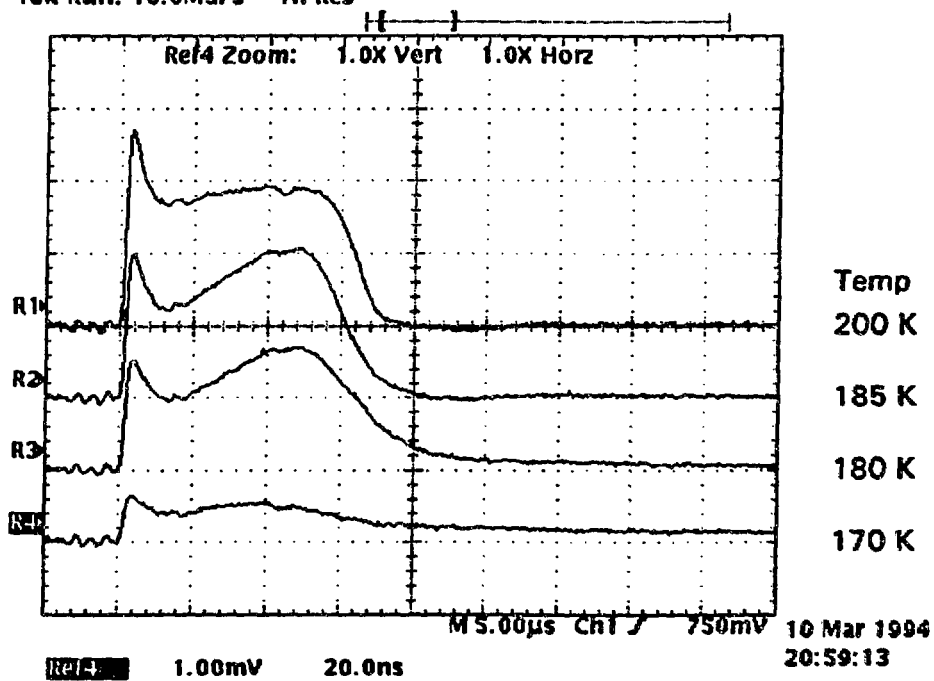
Figure 2

Tek Run: 10.0MS/s HI Res



a)

Tek Run: 10.0MS/s HI Res



b)

Figure 3

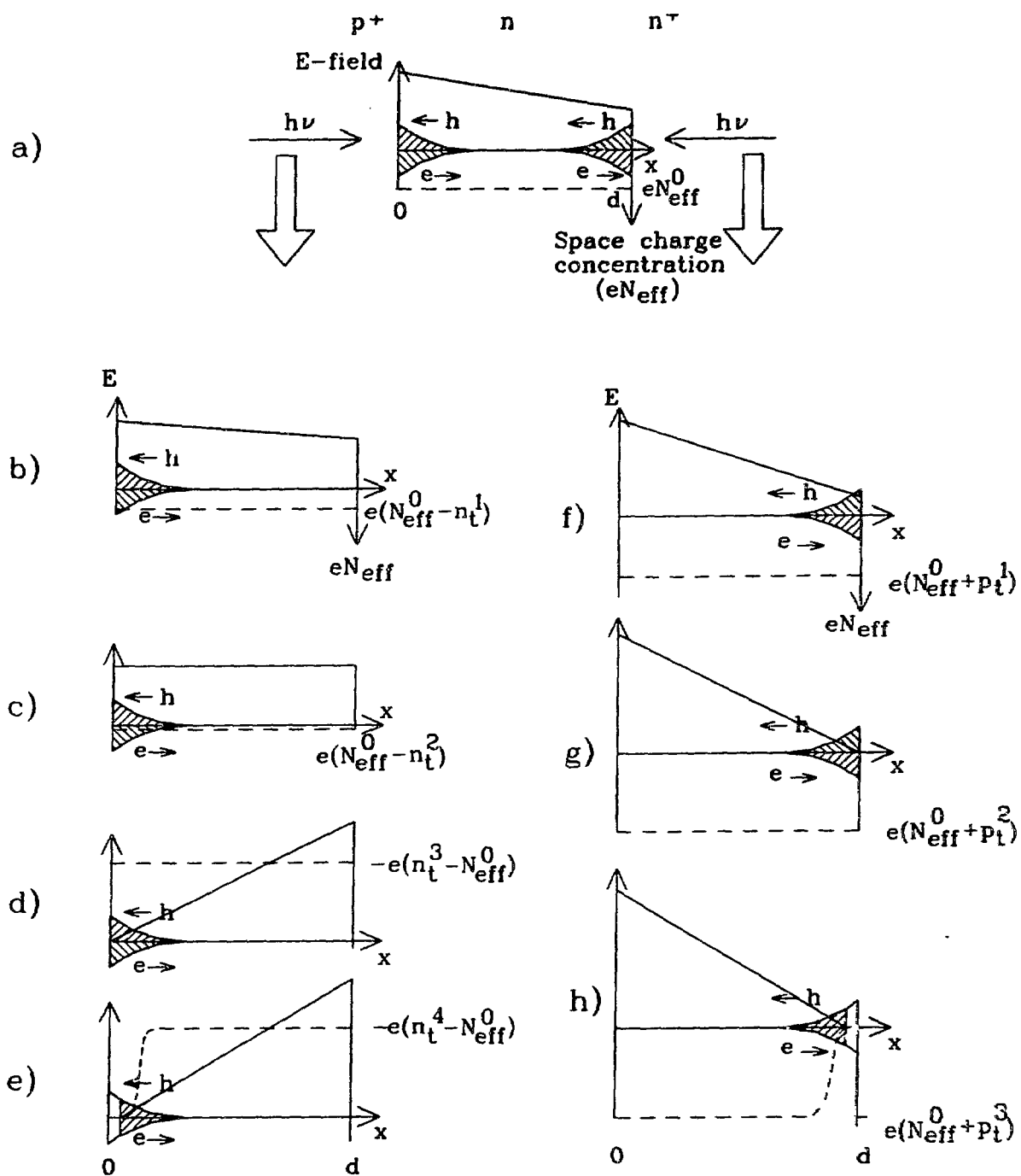


Figure 4

Simulated nt vs. t
 $N_{eff0}=4.6 \times 10^{12} / \text{cm}^3$, $d=600 \text{ } \mu\text{m}$

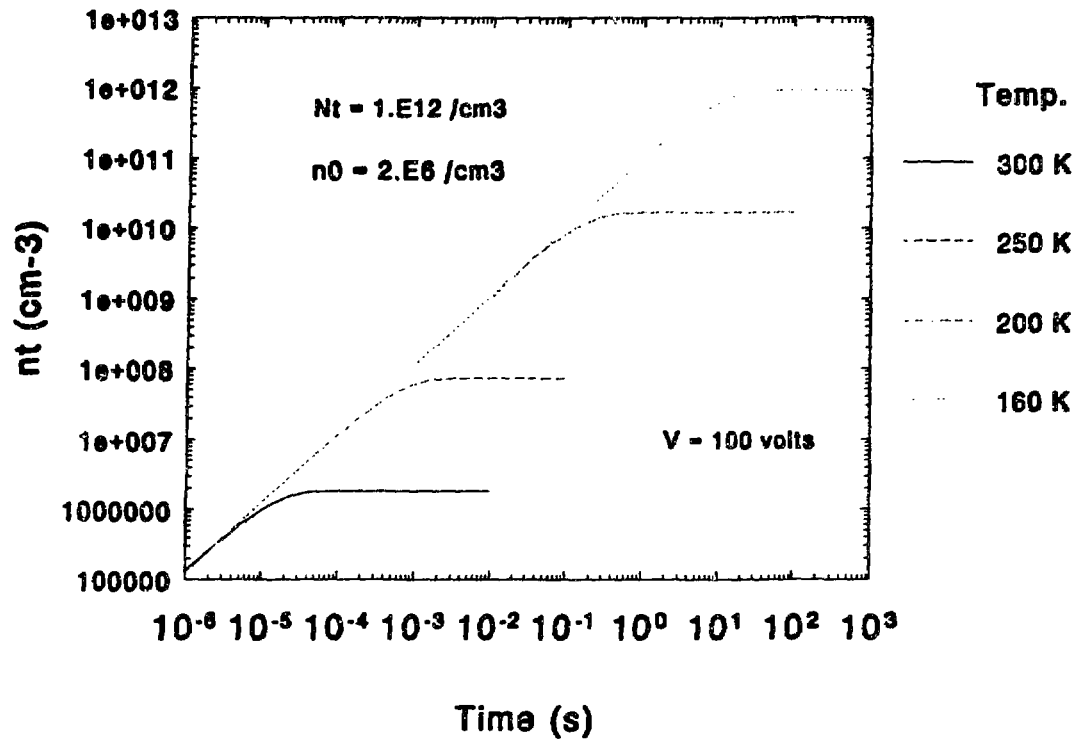
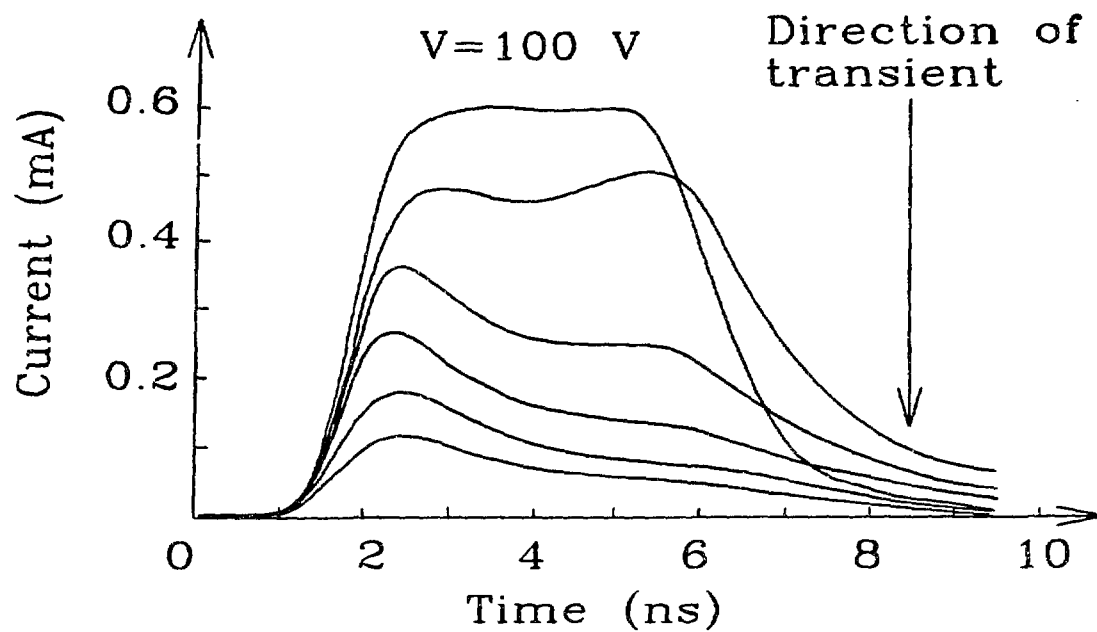
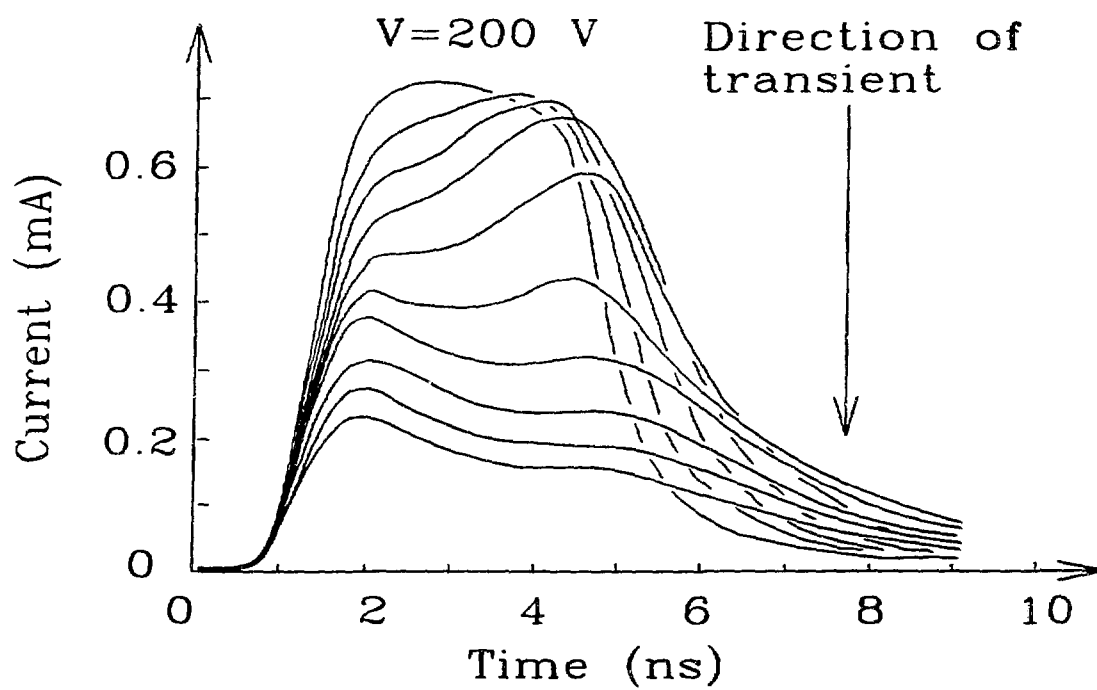


Figure 5



a)

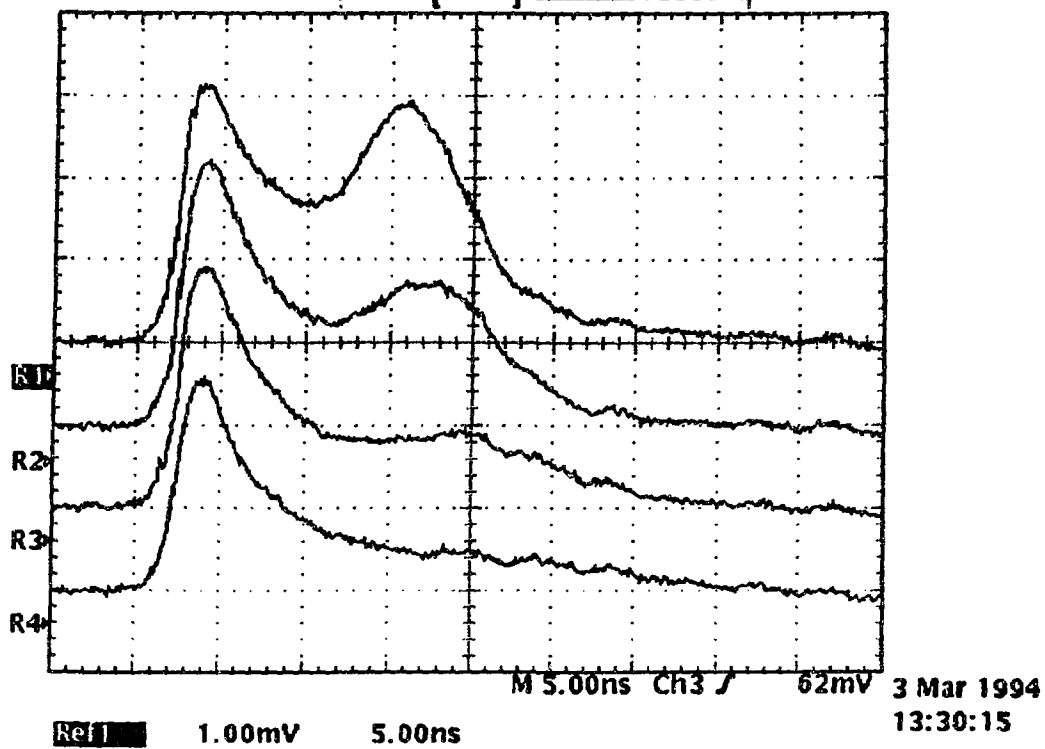


b)

Figure 6

Tek Stop 10.0GS/s ET

0 Acqs



Figur 7